

Insights into Stability of Magnesium Borate Salts for Rechargeable Magnesium Batteries from AIMD Simulations

Shuxin Zhang, Mingxiang Cheng, Peng Zhang, Yaru Wang, Duo Zhang, Yang Yang, Jiulin Wang, Yanna NuLi*

Supporting Information

Computational Detail

All the periodic DFT calculations were performed using CP2K software package¹. The exchange-correlation energy was determined using gradient approximation (GGA) Perdew-Burke-Ernzerhof (PBE) functional² and molecularly optimized double- ζ quality (DZVP) basis sets³ coupled with Grimme's D3-dispersion correction⁴. For the auxiliary plane-wave (PW) basis, we used 300 Ry for the PW energy cutoff and 60 Ry for the reference grid cutoff. Goedecker-Teter-Hutter pseudopotentials^{5, 6}, which are compatible with the employed basis sets, were used for all the elements. Due to the large supercell sizes considered in our simulations, the Brillouin zone integration was performed only at the Γ -point. All optimization calculations were converged until the forces on all atoms were less than 0.02 eV/Å. The AIMD simulations were performed using NVT ensemble at a temperature of 750 K, and these temperatures were maintained using the Nose-Hoover thermostat of chain length 10. The equations of motion were integrated with a 1 fs time step (using a tritium mass for the hydrogen atoms). Time dependent charge-transfer analyses were conducted using Mulliken charges, which were printed at each time step.

In all our simulations, we used supercells of a Mg(001)-surface, which were generated using a symmetrized magnesium unit cell (P63/MMC space group, edge length: $a=b=3.2094$ Å, $c=5.2105$ Å). To study salt-surface interactions, a salt molecule on top of a three-layer, 10×10 -supercell of magnesium (resulting in a 32.094 Å \times 32.094 Å \times 20.2105 Å cell consisting of 300 Mg atoms) was considered. The large supercell size ensures at least 15 Å of distance between the periodic images of salt molecules in both the a and b directions. In addition, we also used a 15 Å vacuum along the c direction to avoid any spurious interactions between the periodic images. Furthermore, to accurately represent the slab configuration, we fixed the coordinates of the bottom layer of the Mg atoms to their bulk values.

Measurements

0.5 M Mg(TFSI)₂/THF, Mg[B(Otfe)₄]₂/THF and Mg[B(Ohfip)₄]₂/THF electrolytes were prepared as reported.⁷⁻⁹ CR2032 experimental coin cells of SS||Mg were assembled with stainless steel (SS) as the cathode, Entek PE as the separator, and magnesium strip polished with coarse sandpaper as the anode in an Ar-filled glove box. The electrochemical magnesium plating/stripping performances in the Mg(TFSI)₂/THF, Mg[B(Otfe)₄]₂/THF and Mg[B(Ohfip)₄]₂/THF electrolytes

were studied via SS||Mg CR2032 experimental coin cell on a battery measurement system (Wuhan, China). The magnesium was first plated on the stainless-steel (SS) substrate at a constant current charge for 30 min and then charged at a constant current density of 0.1 mA cm^{-2} until 0.8 V to strip the magnesium. Each step was left for 30 s between the charging and discharging processes.

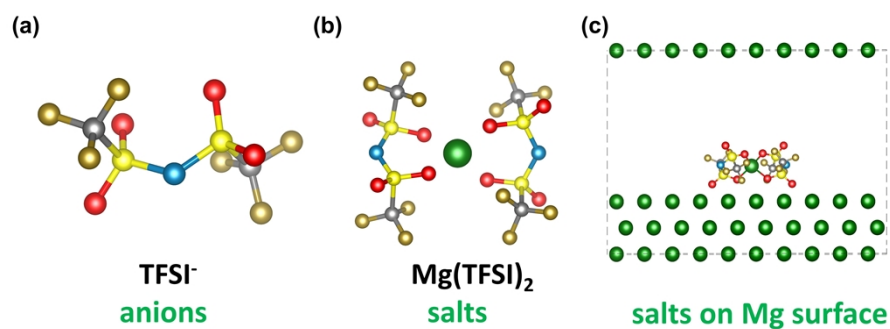


Figure S1. Optimized geometry of (a) TFSI⁻ anion, (b) Mg(TFSI)₂ salt; (c) Mg(TFSI)₂ salt on Mg surface. The color codes for the atoms are dark green: Mg, blue: N, red: O, gray: C, brown: F, and yellow: S.

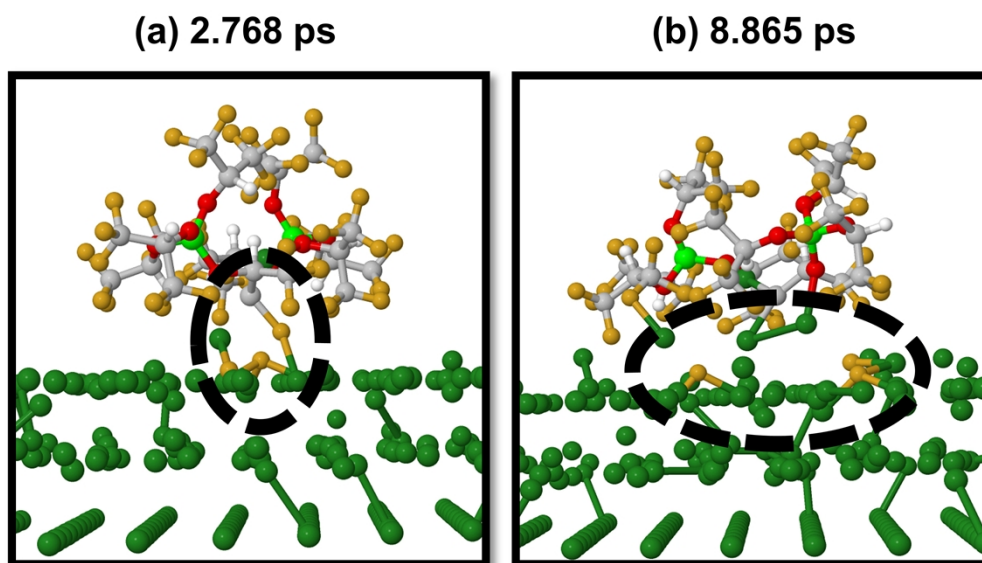


Figure S2. Representative snapshots of Mg[B(Ohfp)₄]₂ on the Mg surface at 2.768 ps (a) and 8.865 ps (b) from AIMD simulations at 750 K. The color codes for the atoms are dark green: Mg, light green: B, red: O, gray: C, brown: F, and white: H. The black dotted circles represent the broken chemical bonds.

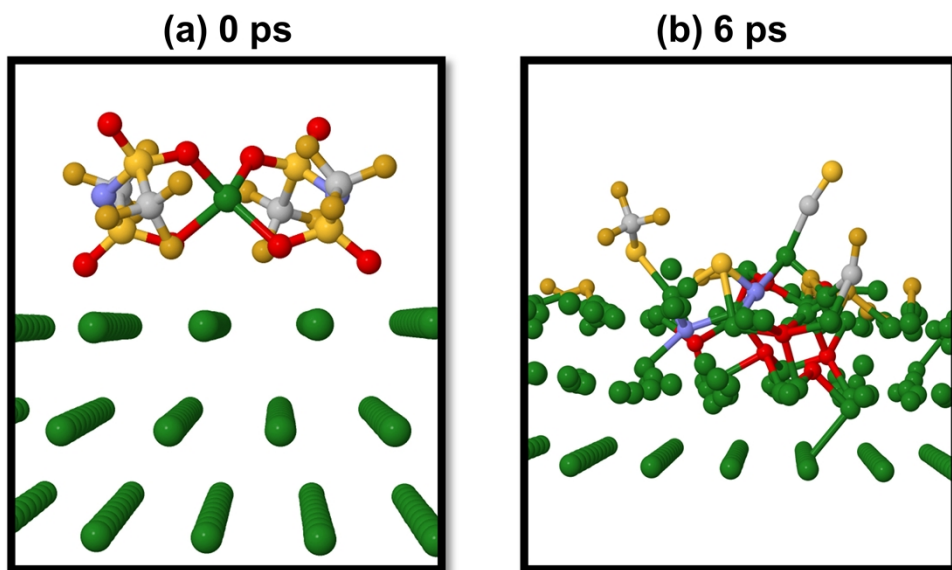


Figure S3. Representative snapshots of $\text{Mg}(\text{TFSI})_2$ on the Mg surface from AIMD simulations at 750 K. The color codes for the atoms are dark green: Mg, purple: N, red: O, gray: C, brown: F, and white: H.

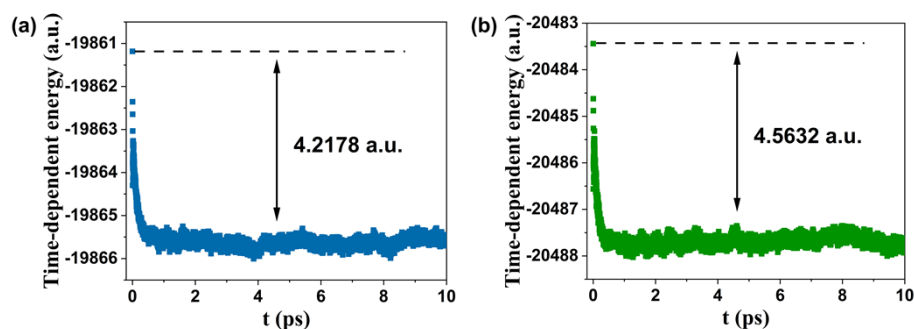


Figure S4. Time-dependent energy trends between (a) $\text{Mg}[\text{B}(\text{Otf})_4]_2$, (b) $\text{Mg}[\text{B}(\text{Ohfip})_4]_2$ and Mg surface at 750 K.

The activation barriers that represent the reaction trends of the $\text{Mg}[\text{B}(\text{Otf})_4]_2$ (Fig. S4a) and $\text{Mg}[\text{B}(\text{Ohfip})_4]_2$ (Fig. S4b) with the Mg anode were obtained by the time-dependent energy. Comparing to $\text{Mg}[\text{B}(\text{Ohfip})_4]_2$, the lower energy barrier (4.2178 a.u.) proves that $\text{Mg}[\text{B}(\text{Otf})_4]_2$ salt can react with the Mg anode more easily on the surface, which further supports the result of the simulations in the Fig. 4.

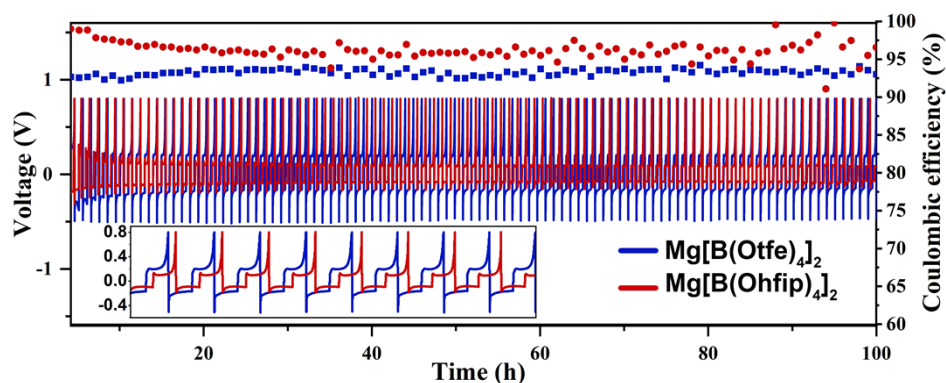


Figure S5. Coulombic efficiency and corresponding voltage-time curves of Mg deposition-dissolution upon cycling in more detail via SS||Mg coin-cells with the electrolytes of 0.5 M $\text{Mg}[\text{B}(\text{Otf})_4]_2$ and $\text{Mg}[\text{B}(\text{Ohfip})_4]_2$ salts in THF solvent at 0.1 mA cm^{-2} .

References:

1. J. VandeVondele, M. Krack, F. Mohamed, M. Parrinello, T. Chassaing and J. Hutter, *Comput. Phys. Commun.*, 2005, **167**, 103-128.
2. J. P. Perdew, K. Burke and M. Ernzerhof, *Phys. Rev. Lett.*, 1996, **77**, 3865-3868.
3. J. VandeVondele and J. Hutter, *J. Chem. Phys.*, 2007, **127**, 114105.
4. S. Grimme, S. Ehrlich and L. Goerigk, *J. Comput. Chem.*, 2011, **32**, 1456-1465.
5. M. Krack, *Theor. Chem. Acc.*, 2005, **114**, 145-152.
6. S. Goedecker, M. Teter and J. Hutter, *Physical Review B*, 1996, **54**, 1703-1710.
7. N. Sa, B. Pan, A. Saha-Shah, A. A. Hubaud, J. T. Vaughey, L. A. Baker, C. Liao and A. K. Burrell, *ACS Appl. Mater. Interfaces*, 2016, **8**, 16002-16008.
8. W. Ren, D. Wu, Y. N. NuLi, D. Zhang, Y. Yang, Y. Wang, J. Yang and J. L. Wang, *ACS Energy Lett.*, 2021, **6**, 3212-3220.
9. Z. Zhao-Karger, M. E. Gil Bardaji, O. Fuhr and M. Fichtner, *J. Mater. Chem. A*, 2017, **5**, 10815-10820.